ELSEVIER

Cosmogenic nuclide chronology of pre-last glacial maximum moraines at Lago Buenos Aires, 46°S, Argentina

Michael R. Kaplan[a,b,*], Daniel C. Douglass[a], Bradley S. Singer[a],
Robert P. Ackert[c], Marc W. Caffee[d]

[a]Department of Geology and Geophysics, University of Wisconsin-Madison, 1215 West Dayton Street, Madison, WI 53706, USA
[b]School of GeoSciences, University of Edinburgh, Edinburgh, EH8 9XP, Scotland, UK
[c]Department of Earth and Planetary Sciences, Harvard University, 20 Oxford Street, Cambridge, MA 02138, USA
[d]Department of Physics, Purdue University, West Lafayette, IN 47907-1396, USA

Abstract

At Lago Buenos Aires, Argentina, ^{10}Be, ^{26}Al, and ^{40}Ar/^{39}Ar ages range from 190,000 to 109,000 yr for two moraines deposited prior to the last glaciation, 23,000–16,000 yr ago. Two approaches, maximum boulder ages assuming no erosion, and the average age of all boulders and an erosion rate of 1.4 mm/10^3 yr, both yield a common estimate age of 150,000–140,000 yr for the two moraines. The erosion rate estimate derives from ^{10}Be and ^{26}Al concentrations in old erratics, deposited on moraines that are >760,000 yr old on the basis of interbedded ^{40}Ar/^{39}Ar dated lavas. The new cosmogenic ages indicate that a major glaciation during marine oxygen isotope stage 6 occurred in the mid-latitude Andes. The next five youngest moraines correspond to stage 2. There is no preserved record of a glacial advance during stage 4. The distribution of dated boulders and their ages suggest that at least one major glaciation occurred between 760,000 and >200,000 yr ago. The mid-latitude Patagonian glacial record, which is well preserved because of low erosion rates, indicates that during the last two glacial cycles major glaciations in the southern Andes have been in phase with growth and decay of Northern Hemisphere ice sheets, especially at the 100,000 yr periodicity. Thus, glacial maxima are global in nature and are ultimately paced by small changes in Northern Hemisphere insolation.
© 2005 University of Washington. All rights reserved.

Keywords: Exposure age; Cosmogenic nuclide; South America; Glacial geology; Paleoclimatology; Glaciation; Southern Hemisphere; Milankovitch; Quaternary period; Stage 6

Introduction

Understanding the causes of the Pleistocene ice age requires firm chronologic data on the growth and decay of glaciers in both hemispheres at all time scales. Glacier records are vital because they provide a proxy for temperature and precipitation. Well-dated glacial moraine records from the Southern Hemisphere can be used to evaluate hypotheses that explain how orbital-paced changes in solar insolation in the Northern Hemisphere pace global climate changes, and the relative roles of atmospheric cooling, ocean circulation, and sea level change (Broecker and Denton, 1989; Imbrie et al., 1993; Mercer, 1983). For example, such data can help determine whether the 100,000-year periodicity in the mid- to Late Quaternary paced large ice sheets and smaller mountain glacial systems in both hemispheres, which is not necessarily predicted from Milankovitch theory (Hays et al., 1976).

Despite their value for understanding former climate change and the Pleistocene ice age, directly dated terrestrial records prior to ca. 25,000 yr ago (marine oxygen isotope stage 2) are rare. The paucity of chronologic data largely reflects the 40,000-yr limit of radiocarbon dating. Cosmogenic surface exposure dating has the potential to resolve the timing of glacial events much older than 40,000 yr ago. Under suitable conditions, this method has been used to define glacial changes prior to 100,000 yr ago in Antarctica, western North America, and eastern Africa (e.g., Brook et al., 1993; Phillips et al., 1997; Shanahan and Zreda, 2000).

* Corresponding author. School of GeoSciences, University of Edinburgh, Edinburgh, EH8 9XP, Scotland, UK. Fax: +44 131 650 2524.
E-mail address: mkaplan@geo.ed.ac.uk (M.R. Kaplan).

The dry steppe in the rain shadow of the Andes provides ideal conditions for applications of surface exposure techniques (Ackert et al., 2003; Kaplan et al., 2004). The glacial record adjacent to Lago Buenos Aires, Argentina (LBA, Fig. 1), 46.5°S, comprises one of the most complete and intact sequences of Quaternary moraines in the world (Clapperton, 1993). Prior research has focused on magnetic polarity of the glacial sediments (Mörner and Sylwan, 1989), $^{40}Ar/^{39}Ar$ and K–Ar dating of basalt flows interbedded with the glacial deposits, providing a chronological framework for the ~1 myr record (Singer et al., 2004), and cosmogenic dating of the youngest, <25,000-yr-old, moraines (Kaplan et al., 2004). In this paper, exposure ages are presented for glacial deposits older than the last glacial maximum (>25,000 yr ago). The chronology demonstrates that a major mountain glaciation occurred during marine oxygen isotope stage 6 in Patagonia and indicates that Quaternary ice age maxima are global in nature despite spatial differences in solar insolation (Berger and Loutre, 1991).

Setting and methods

Surficial geologic mapping has delineated evidence of at least 19 moraines, associated outwash plains, and three inter-
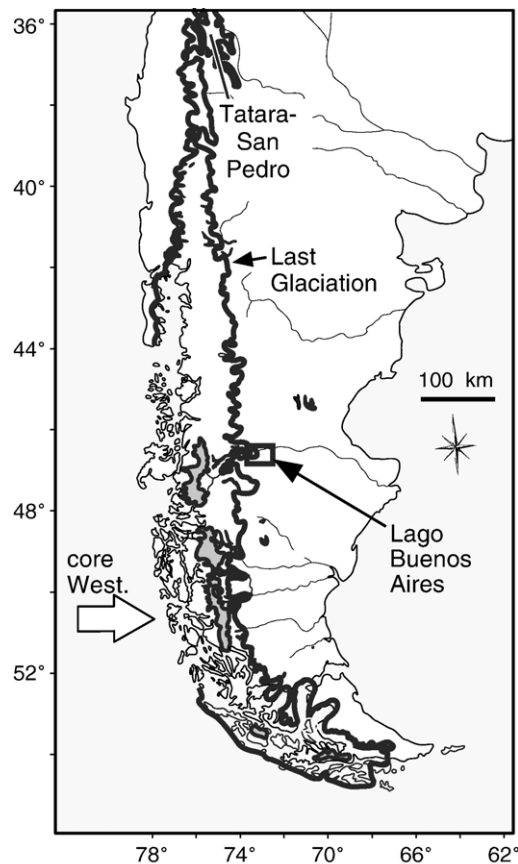

Figure 1. Location of Lago Buenos Aires (LBA), referenced place names, present ~latitude of the core of the Southern Hemisphere Westerlies, and glacial extent during the last glaciation as originally mapped by Caldenius (1932).

bedded lava flows deposited east of LBA (Fig. 2). Singer et al. (2004) described the surficial geology in detail and presented $^{40}Ar/^{39}Ar$ ages of the lava flows that provide chronologic control for the 1 myr glacial sequence; hence, we highlight only the salient aspects of the record. The moraines are grouped into four broadly defined moraine complexes, which are informally named Fenix, Moreno, Deseado, and Telken, that are separated by prominent ~50–100 m escarpments (Fig. 2). The oldest glacial deposit at LBA, Telken VII, is the equivalent of the greatest Patagonian glaciation (Mercer, 1983), which is constrained in age to between 1.168 and 1.016 myr based on the $^{40}Ar/^{39}Ar$ age of the local overlying Arroyo Telken Flow (Fig. 2) and the underlying Bella Vista lava flow in the southern Santa Cruz province (Singer et al., 2004). The Telken VII–I moraines were deposited between 1.016 myr and the eruption of the 760,000 yr Arroyo Page Flow, and the Deseado and Moreno moraines between 760,000 and the 109,000 yr old Cerro Volcán Flow (Singer et al., 2004). In situ cosmogenic ^{10}Be, ^{26}Al, and ^{3}He, and ^{14}C ages, indicate that the Fenix V–I moraines were deposited between ca. 23,000 and 16,000 yr ago (Kaplan et al., 2004). Here, the ages of the Moreno and Deseado moraine complexes are further constrained with cosmogenic dating.

The Telken and Deseado moraines are broader features compared to the younger, more sharply crested Moreno and Fenix moraines. Desert pavement is best developed on Telken VII, although it is found sporadically on younger moraines. Telken IV is the highest and largest of the glacial landforms expressed at the surface at LBA. The Moreno moraines more commonly have identifiable closed depressions (Fig. 3B; e.g., kettle holes), in contrast to older moraines. Moreno III is far less continuous than Moreno I and II (Fig. 2), which may be due to glacio-fluvial erosion associated with later Moreno glacial events (Fig. 3C). In at least one place, near Route 43, a Moreno II crest cross-cuts a Moreno III crest. Outwash graded to the Moreno I moraine forms a discontinuous terrace at about 460–440 masl along the south side of the Rio Deseado valley (Figs. 2 and 3A). This terrace is buried by the Cerro Volcán basalt flow, and thus the Moreno system is older than the 109,000-yr-old lava (Singer et al., 2004). Erratics of granite, rhyolite, diorite, basalt, gneiss, schist, and other lithologies derived from the Andean Cordillera >50 km to the west are found on the moraines.

Cosmogenic surface exposure dating

Sampling

The geomorphic setting and boulder characteristics were considered carefully when choosing samples, which were deemed the best available from a given locality. Boulders with evidence of splitting or exfoliation were avoided. Moreno boulders commonly exhibit ventifaction, which is found less often on older moraines (Fig. 3D). In comparison, boulder exfoliation and splitting are relatively uncommon on Moreno moraines, but are found occasionally on Deseado and Telken moraines (Fig. 3E). We preferentially selected the
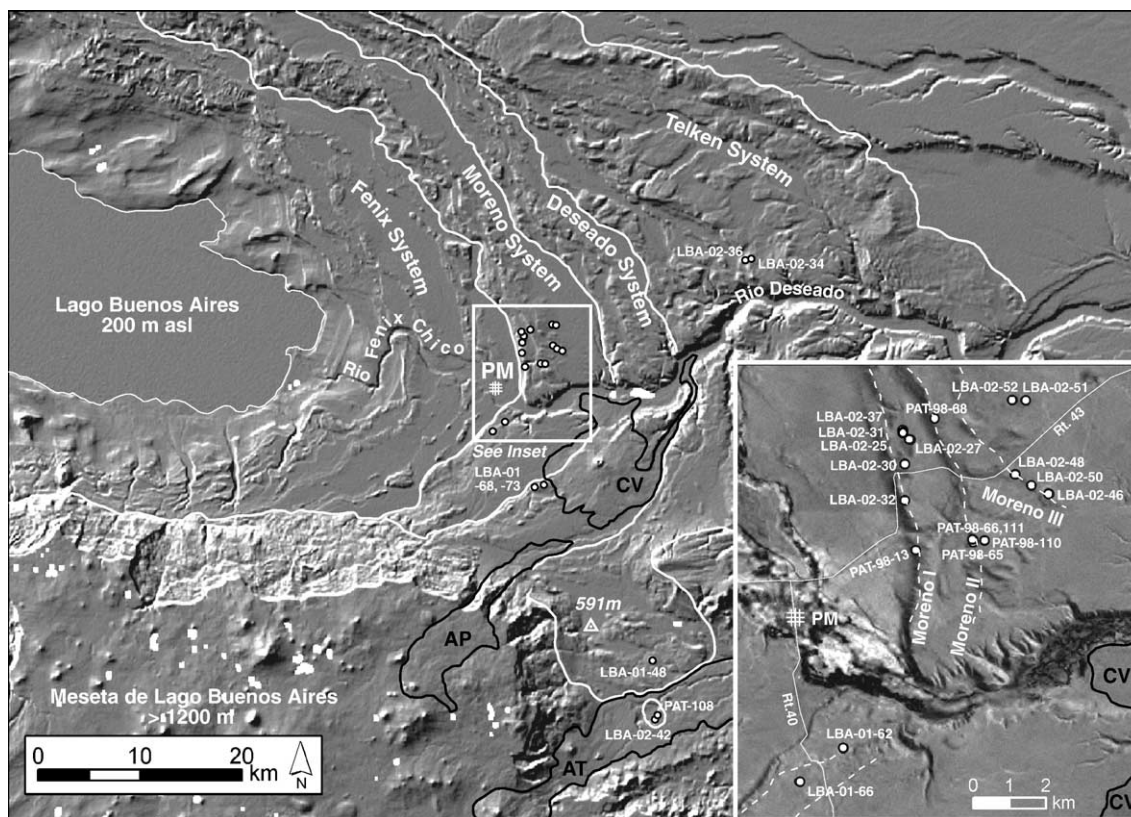
Figure 2. A digital hill shade of 90 m Shuttle Radar Topography Mission (SRTM) elevation dataset showing the main moraine systems east of Lago Buenos Aires, sample locations, and lava flows. Inset shows details of Moreno I, II, and III samples and other features mentioned in the text, on a Landsat image. CV = Cerro Volcán flow ($109,000 \pm 3000$ yr), AP = Arroyo Page flow ($760,000 \pm 14,000$ yr), AT = Arroyo Telken flow (1.016 ± 0.01 myr), (lava flow ages $\pm 2\sigma$). PM = town of Perito Moreno. The 591 m asl benchmark (triangle) is on Estancia Telken.

largest boulders on, or nearly on, moraine crests, which are believed to be stable and to have stood above snow or volcanic ash. The full range in boulder height varies from 5 to 200 cm (Appendix Table A1). The shortest boulders (those <75 cm tall) were sampled out of necessity, especially south of the Rio Fenix Chico (Fig. 2), where larger boulders were not found. We tried to sample a common granitic lithology (Appendix Table A1), but this was not possible in all cases. Samples were collected from the upper few cm of moraine boulders, at least 5 cm from edges and sharp facets, with hammer and chisel. Elevations were measured relative to a 591-m benchmark (Fig. 2) using a barometric-based altimeter (analytical precision ± 0.1 m), cross-checked against GPS and topographic maps, and are estimated to be within 10–20 m. Snow cover is not corrected for, but it is assumed to be insignificant on moraine crests (<1% change to exposure ages; mean annual precipitation is 250 mm and appreciable accumulation usually lasts less than a month). In glacial periods, snow accumulation may have lasted longer, but modeling experiments suggest that the climate may have been drier (Sugden et al., 2002).

Quartz was separated and purified at the University of Wisconsin using standard methods (Bierman et al., 2002). Ion-exchange chromatography and precipitation techniques chemically isolated Be and Al. Stable Al was measured by inductively coupled plasma atomic emission spectroscopy (ICP-AES) at the University of Colorado-Boulder. All $^{10}\text{Be}/^{9}\text{Be}$ and $^{27}\text{Al}/^{26}\text{Al}$ isotope ratios were measured at Purdue University's PRIME Lab, except for three samples from Kaplan et al. (2004), which were measured at the Center of Accelerator Mass Spectrometry at Lawrence Livermore National Laboratory (LLNL). $^{10}\text{Be}/^{9}\text{Be}$ ratios from PRIME Lab were increased by 14% to account for the use of standards derived from the National Institute of Standards and Technology (NIST) SRM 4325, which yields a lower ^{10}Be mean-life than that previously accepted by many researchers (see note 34 in Partridge et al., 2003; Middleton et al., 1993). The 14% adjustment allows comparison to ratios from other AMS facilities, including LLNL. Details of the ^{3}He sample LBA-98-134 were presented in Kaplan et al. (2004).

Production rates

Systematic uncertainties associated with production rates of cosmogenic nuclides, including scaling to latitude and altitude, are usually estimated to be 10–20% (Gosse and Phillips, 2001) and would provide constraints on interpreting exposure ages on the time scales discussed here. Use of a locally determined, long-term production rate reduces uncertainties towards analytical precision of calibration measurements. The production rate we use is based on ^{3}He concentrations in the $^{40}\text{Ar}/^{39}\text{Ar}$ and K–Ar dated Cerro Volcán
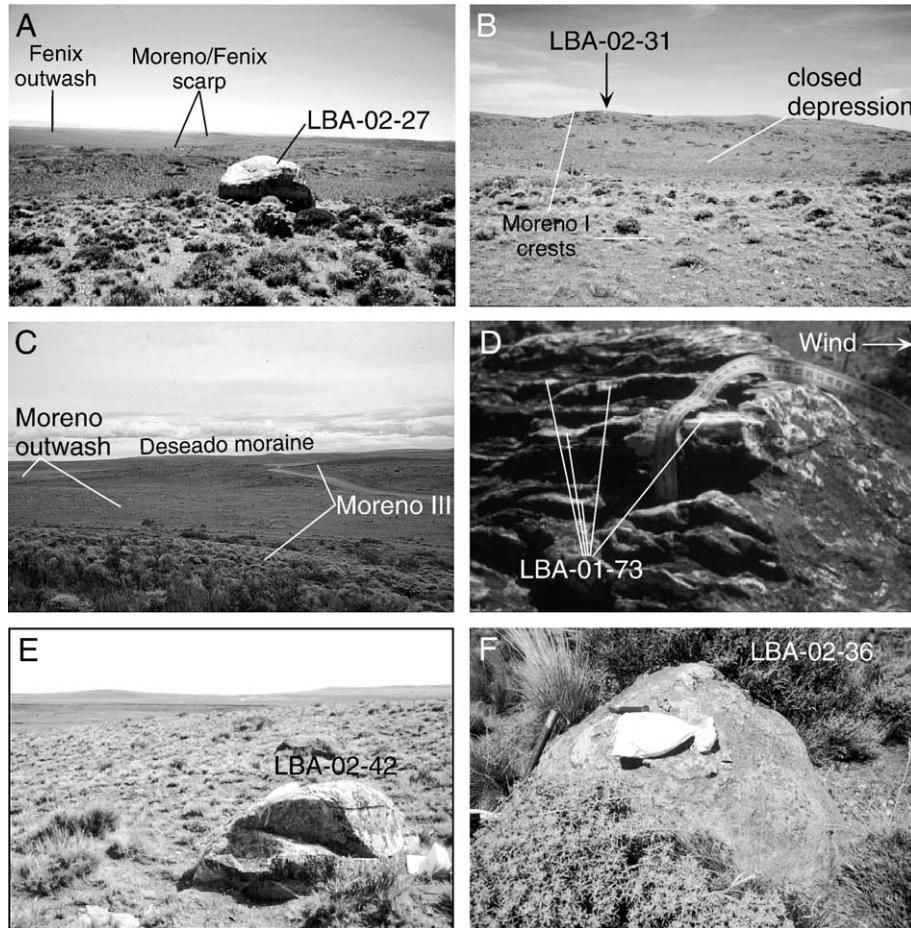
Figure 3. Photographs of Moreno, Deseado, and Telken moraines. (A) From Moreno I, shown are the scarp separating the Fenix and Moreno systems and Fenix outwash plain. (B) Looking north on a Moreno I crest, with a closed depression. Location of LBA-02-31 shown. (C) Looking east from a Moreno III crest. Deseado moraine in background. (D) LBA-01-73, a relatively low 25-cm-tall boulder on Deseado I. Lines point to sampled spots and tape measure provides scale. (E) Looking northeast on broad flat-topped Telken VII. Note splitting of ~50 cm high LBA-02-42. (F) Close-up of LBA-02-36. Note boulder surface relief.

and Rio Pinturas lava flows (109,000 and 69,000 yr), which are of a similar elevation (900 and 500 m; Ackert et al., 2003) and location (within 50 km) with respect to the moraines. These two lava flows indicate a ^{3}He production rate ~11% higher than published "global" values (Ackert et al., 2003; Licciardi et al., 1999) over the last 109,000 yr, taking into account modern atmospheric temperature and pressure at LBA (Stone, 2000). The higher rate over the last 109,000 yr is primarily attributed to northward movement of the Antarctic Polar Front and lower atmospheric pressure at LBA during glacial periods (Ackert et al., 2003). The local production rate includes effects of magnetic field variations and changes in atmospheric pressure for the last ~109,000 yr. We assume that this production rate should also be applicable to the older boulders of the Deseado and Telken moraines because changes in the effective geomagnetic latitude between 100,000 yr and 1 myr are <1° (cf. Gosse and Phillips, 2001) and the production rate integrates atmospheric pressure over ~one glacial–interglacial cycle. Because ^{3}He, ^{10}Be, and ^{26}Al are all produced dominantly by spallation (Gosse and Phillips, 2001), we increase the other (spallation) production rates accordingly by ~11%. In addition, a muon component of

2.6% and 2.2% of total production is assumed for ^{10}Be and ^{26}Al, respectively (Stone, 2000).

For comparison, ages are also presented with global production rates of 5.1 and 31.1 atoms g^{-1} yr^{-1} for ^{10}Be and ^{26}Al, respectively (sea level, high latitude; Gosse and Stone, 2001; Stone, 2000), corrected for a local air pressure of 1009.32 mbar and annual temperature of 285 K (Table 2). As described in Kaplan et al. (2004), use of global production rates at LBA may require scaling to an effective geomagnetic latitude to compensate for changes in the magnetic field over a sample's exposure history (Nishiizumi et al., 1989). For moraines much older than 25,000 yr, a theoretical estimate of the impact on total production rates is <0.5% (Masarik et al., 2001) whereas the correction outlined by Nishiizumi et al. (1989) and Gosse and Phillips (2001), which is used here, increases production rates by <4% (Kaplan et al., 2004).

Boulder erosion rate

Given the antiquity of the deposits, some scatter in the data is expected due to spatial and temporal variability in erosion rates and the possibility of post-depositional movement causing rotation, burial, or exhumation (Putkonen and

Swanson, 2003). Erosion and boulder exhumation are the largest geologic uncertainties in this study. Erosion rate becomes an increasingly larger factor over time, as shown by a non-linear age equation (Lal, 1991):

$$t = \frac{\ln\left(1 - \frac{N\left(\lambda + \frac{E}{L}\right)}{P}\right)}{-\left(\lambda + \frac{E}{L}\right)} \qquad (1)$$

where N is nuclide concentration, P is production rate, E is erosion rate, λ is the decay constant, and L is the attenuation length in the rock. Although we have constrained boulder erosion rates (see below), the occurrence of exhumation must be inferred with sample redundancy to identify outliers and comparison to limiting lava flow ages.

Erosion rate may have varied spatially, temporally, and with rock type. To estimate erosion rate and its variability throughout the area, we measured the concentrations of ^{10}Be and ^{26}Al in glacial erratics of similar lithologies on the old Telken moraines (Fig. 2; Appendix Table A1). Using the independent ^{40}Ar/^{39}Ar age constraints for these deposits, we solved for erosion rate given the ^{10}Be and ^{26}Al isotope concentrations, respectively. In all cases, the zero-erosion exposure ages of the boulders are significantly lower than the minimum 760,000 yr age of the Telken landforms (Table 1). Boulder erosion rates are partly a function of the production rate used (Eq. 1). The local long-term production rate (Ackert et al., 2003) generates erosion rates ~10–30% higher than those derived with the rates of Stone (2000).

Three important assumptions with using Telken boulder nuclide concentrations to evaluate erosion rates at LBA are: (1) the Telken boulders have been at the moraine surface since deposition. If the boulders were exhumed, then the exposure age should be less than the landform age and the calculated erosion rates will be higher than the actual erosion rate. (2) All boulders have a similar fracture or exfoliation history and flake thickness has been insignificant. For a given Telken boulder, fracturing is taken into account by the average erosion rate, however, the disintegration history of individual boulders is different. And (3) erosion rates have remained spatially constant over the LBA region and between different lithologies. Although we recognize the assumptions and limitations in deriving erosion rates on old boulders and inferring that similar rates affected younger boulders, our estimates are consistent and help to place upper limits on the potential impact that erosion may have in this region (Fig. 4).

Final age calculation and errors

Exposure ages are shown with analytical uncertainties and with uncertainties propagated step-by-step as we solved the respective age equations (Taylor, 1982) (all errors $\pm 1\sigma$; Table 2). Propagated uncertainties, assumed to be random, include those associated with accelerator mass spectrometry, ICP-AES analyses of Al concentration (4%), erosion rate (~10%), and attenuation length (4.8% and 8.0% for ^{10}Be and ^{26}Al, respectively, Brown et al., 1992). In terms of systematic

uncertainties, those for ^{10}Be and ^{26}Al production rates are ~3% ($\pm 1\sigma$) based on Stone (2000). For ages estimated with global production rates, our errors do not include uncertainties for scaling to latitude, altitude, and estimated geomagnetic field changes, which could be >10% (e.g., Gosse and Phillips, 2001). Total errors on the ages after step-by-step propagation of the above errors are for ^{10}Be, 16–20% and 27–40% at 150,000 and 500,000 yr, respectively, and for ^{26}Al, ~24–33% and ~45% at 150,000 and 500,000 yr, respectively.

For boulder and moraine ages, we average data instead of calculating inverse variance-weighted means for the following reasons. First, it cannot be assumed that 'old' (e.g., >25,000 yr) age distributions such as presented here have Gaussian characteristics (Hallet and Putkonen, 1994; Zreda and Phillips, 1995) because of unknown spatial and temporal variability of geologic effects such as boulder erosion and exhumation. Second, because uncertainties are propagated step by step, older ages always have higher uncertainties, causing younger ages to influence strongly weighted mean calculations.

Results

Boulder erosion

Erosion rates on Telken boulders are consistently less than 2.4 mm/10^3 yr (Table 1; Fig. 4). One exception, LBA-98-108, is at the top edge of a sloped surface with no vegetation that appears eroded from recent sheet wash; we infer that it was more recently exhumed than the other samples and this sample is not discussed further. Also, the LBA-01-48 ^{26}Al-erosion rate is not considered because of the large analytical AMS uncertainty (30%). Samples LBA-02-34 and 36 are on the same crest in the northeast part of the study area and produce erosion rates of <1.3 mm/10^3 yr, whereas those to the southeast (Fig. 2) are eroding slightly faster, <2.4 mm/10^3 yr. For Telken IV and V, the calculated erosion rates are about 10% different if one assumes limiting ages for these old boulders of 760,000 yr versus 1.016 myr (from the ^{40}Ar/^{39}Ar ages of the lava flows bracketing moraines on which these boulders rest; Table 1; Singer et al., 2004). This ~10% error is propagated into the age equation (see above). In addition, the erosion rates are nearly the steady state values (Table 1), where nuclide accumulation is equal to loss by radioactive decay and erosion (Lal, 1991), indicating that they are close to maximum values for these particular boulders. The average erosion rate of the Telken boulders is 1.4 mm/10^3 yr (Table 1). This value excludes the high ratio sample LBA-02-42; however, if this boulder is included in the average, the rate would be similar, 1.5 mm/10^3 yr.

To illustrate the magnitude of the possible effect on erosion rates if the Telken boulders were exhumed after moraine deposition, let us assume that Telken boulders have been exposed for 500,000 years. In this scenario, on average the ^{10}Be and ^{26}Al based erosion rates decrease by ~30% and

Table 1
Erosion rate constraints from ^{10}Be and ^{26}Al data at Lago Buenos Aires

Sample	Boulder height (cm)	^{10}Be	^{26}Al	$^{26}Al/^{10}Be$	Age (10^3 yr)[a]		^{10}Be erosion rate (mm/10^3 yr)				^{26}Al erosion rate (mm/10^3 yr)				Boulder erosion rate[b]
		(10^5 atoms g^{-1})			^{10}Be	^{26}Al	^{10}Be[c]	^{10}Be[d]	±1σ	Steady state	^{26}Al[c]	$26Al$[d]	±1σ	Steady state	
Telken IV															
LBA-02-34	17–30	34.6 ± 0.9	214 ± 12	6.2 ± 0.4	356	400	1.2	1.3	0.1	1.4	1.0	1.1	0.1	1.2	1.2
LBA-02-36	45–55	43.2 ± 1.2	252 ± 15	5.8 ± 0.4	452	490	0.8	0.9	0.2	1.1	0.6	0.8	0.2	0.9	0.8
Telken V															
LBA-01-48	25	22.3 ± 0.5	89.2 ± 13	4.0 ± 1.2	228	153	2.2	2.2	0.1	2.3	*3.6*	*3.7*	*1.1*	*3.9*	2.2
Telken VII															
LBA-02-42	45	21.1 ± 1.0	186 ± 22	8.8 ± 1.1	215	348	–	2.4	0.1	2.4	–	1.4	0.2	1.4	*1.9*
PAT-98-108	30–35	10.4 ± 0.4	82.9 ± 16	7.9 ± 1.6	103	140	–	*5.2*	*0.2*	*5.2*	–	*4.0*	*0.8*	*3.6*	
Average															**1.4**

All samples measured at PRIME Lab except LBA-01-48 (Kaplan et al., 2004). For Telken IV and V samples, ±1σ is the difference between the erosion rates in the two left columns (all values rounded off), which is always higher than the analytical errors (<6%), except for LBA-01-48 ^{26}Al. For Telken VII samples, ±1σ is the analytical uncertainty. All erosion rates calculated with local production rate. Erosion rates in italics are considered outliers for reasons discussed in the text. In addition, LBA-02-42 is italicized because the $^{26}Al/^{10}Be$ ratio is greater than expected at the 95% confidence level.
[a] Age with no erosion.
[b] Average of ^{10}Be and ^{26}Al erosion rates for each boulder, excluding those in italics. An average erosion rate for the boulders is 1.4 mm/10^3 yr (in bold), which is used for Age 2 in Table 2. The value 1.4 mm/10^3 yr excludes the high ratio sample LBA-02-42; however, if this boulder is included in the average, the rate is only slightly higher, 1.5 mm/10^3 yr. The uncertainty for samples included in the average of 1.4 mm/10^3 yr is ~9% and 12% for ^{10}Be and ^{26}Al, respectively.
[c] Based on Arroyo Page Flow age of 760,000 yr.
[d] For Telken IV and V, the erosion rate is based on Arroyo Telken Flow age of 1.016 myr. For Telken VII, the erosion rate is based on an age of 1.092 myr, which is the average age of Arroyo Telken and Bella Vista Flows (Singer et al., 2004).

50%, respectively. A 30% lowering of erosion rate reduces exposure ages of 150,000 and 300,000 yr by <7% and 15%, respectively.

Two Moreno III samples and one Deseado sample provide supporting evidence of erosion rates less than ~2 mm/10^3 yr at LBA. If an erosion rate of >1.4 mm/10^3 yr is used with Moreno III sample LBA-02-46 ^{10}Be nuclide concentrations, the age equation produces an infinite result. On the other hand, assuming that LBA-02-46 has eroded ~1.26 mm/10^3 yr yields a ^{10}Be age of ca. 760,000 yr (Table

Figure 4. Telken boulder erosion rates from Table 1. Not shown are the LBA-98-108 rates, as this sample is on the edge of the deposit and may have been recently exhumed, and the ^{26}Al-based rate of LBA-01-48, which has a large ~30% AMS uncertainty (see text). In addition, nuclide concentrations in Moreno III and Deseado samples LBA-02-46, 52, and LBA-01-68 indicate erosion rates <1.9 mm/10^3 yr.

2), the limiting $^{40}Ar/^{39}Ar$ age, indicating that this is an upper limit on the rate of erosion for this sample. Similarly, given the maximum possible exposure age of 760,000 yr for Moreno III sample LBA-02-52 and Deseado sample LBA-01-68, maximum erosion rates are ~1.8 and 1.7 mm/10^3 yr, respectively, and rates >1.9 mm/10^3 yr result in infinite ages.

Exposure ages

Assuming an erosion rate of 0 mm/10^3 yr, ^{10}Be and ^{26}Al ages from the Moreno I moraine range from 146,000 to 74,000 yr and 157,000 to 95,000 yr, respectively, and from the Moreno II moraine from 153,000 to 80,000 yr and 148,000 to 81,000 yr (Table 2; Fig. 5A), respectively. The young <50,000-yr concordant ages obtained from LBA-02-25 ^{10}Be and ^{26}Al measurements suggest that this ~25-cm-high boulder was exhumed long after moraine formation and it is not considered in determining the moraine age. The maximum ^{10}Be and ^{26}Al ages for Moreno I and II are indistinguishable at 1σ. Individual boulder ages for Moreno I and II, based on the arithmetic mean of the respective ^{10}Be and ^{26}Al ages of the sample, range from 143,000 to 92,000 yr and 150,000 to 80,000 yr, respectively (Tables 2 and 3).

An important result is that Moreno I and II boulder age distributions are similar (Fig. 5). Moreno II has a slightly greater age range and spread of values than Moreno I. Regarding possible exhumation of Moreno I and II boulders, in a broad sense, it appears that the highest samples are more likely to produce the oldest ages (Table 2). For example, on Moreno II, PAT-98-66 is the youngest age, which is the second shortest boulder. However, the Moreno I and II ages are not always simply related to boulder height and it cannot
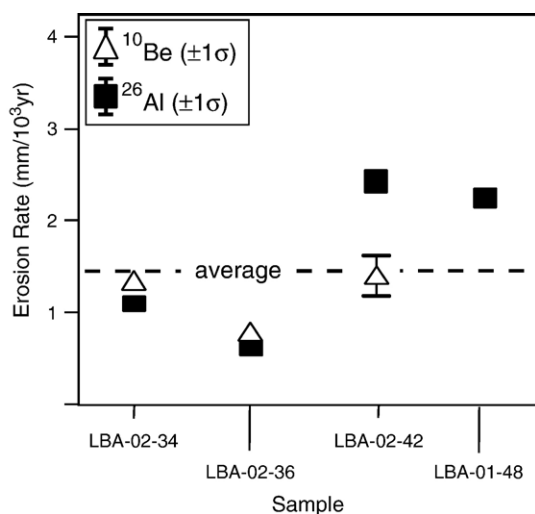
Table 2
^{10}Be and ^{26}Al data from moraine boulders at Lago Buenos Aires 46.5°

Sample	Boulder height (cm)	^{10}Be	^{26}Al	^{26}Al/^{10}Be	Age1 (10^3 yr)[a] Local PR and no erosion		Age2 (10^3 yr)[b] Local PR and no erosion		Age3 (10^3 yr)[a] Global PR and no erosion		Boulder age (10^3 yr)	
		(10^5 atoms g^{-1})			^{10}Be	^{26}Al	^{10}Be	^{26}Al	^{10}Be	^{26}Al	No erosion	Erosion
Moreno I												
LBA-02-25	25	2.72 ± 0.19	25.0 ± 2.4	9.2 ± 1.1	29.2 ± 2.0	44.7 ± 4.6	30.4 ± 5.1	47.3 ± 11	32.0 ± 2.2	49.0 ± 5.1	37.0 ± 11	38.8 ± 12
LBA-02-27	~200	7.38 ± 0.36	82.5 ± 8.4	11 ± 1.3	81.0 ± 4.0	**157** ± 17	90.8 ± 16	199 ± 58	88.9 ± 4.4	173 ± 19	119 ± 54	145 ± 76
LBA-02-30	12–37	8.13 ± 0.79	56.6 ± 3.3	7.0 ± 0.8	88.2 ± 8.6	103 ± 7.4	100 ± 20	119 ± 29	96.7 ± 9.4	114 ± 8.1	95.8 ± 11	110 ± 14
LBA-02-31	130	10.5 ± 0.38	78.9 ± 4.8	7.5 ± 0.5	118 ± 4.2	151 ± 11	141 ± 25	190 ± 50	129 ± 4.6	167 ± 12	135 ± 24	165 ± 35
LBA-02-37	42–63	6.70 ± 0.19	59.1 ± 4.3	8.8 ± 0.7	73.6 ± 2.1	110 ± 9.1	81.6 ± 13	129 ± 32	80.7 ± 2.3	121 ± 10	91.9 ± 26	105 ± 33
PAT-98-13	40	13.1 ± 0.47	74.3 ± 3.6	5.7 ± 0.3	**146** ± 5.2	140 ± 8.8	183 ± 34	172 ± 44	160 ± 5.7	155 ± 9.7	**143** ± 3.9	178 ± 8
LBA-01-62	18–20	11.5 ± 0.27	67.6 ± 1.6	5.9 ± 0.2	133 ± 3.1	132 ± 6.2	164 ± 29	160 ± 39	147 ± 3.4	146 ± 6.8	133 ± 0.76	162 ± 2.5
LBA-01-66	3–5	9.37 ± 0.22	50.0 ± 1.6	5.3 ± 0.2	106 ± 2.4	94.7 ± 4.8	124 ± 21	108 ± 25	117 ± 2.7	104 ± 5.3	100 ± 8.1	116 ± 12
Moreno II												
PAT-98-65	90	13.7 ± 0.57	78.4 ± 4.3	5.7 ± 0.4	**153** ± 6.3	**148** ± 10.0	195 ± 37	185 ± 48	168 ± 7.0	163 ± 11	**150** ± 3.3	190 ± 7
PAT-98-66	70	7.25 ± 0.18	44.1 ± 2.6	6.1 ± 0.4	79.7 ± 1.9	80.9 ± 5.7	89.1 ± 15	90.0 ± 21	87.4 ± 2.1	88.9 ± 6.3	80.3 ± 0.85	89.6 ± 0.61
PAT98-068	60	11.6 ± 0.84	56.8 ± 3.6	4.9 ± 0.5	125 ± 9.0	102 ± 7.7	151 ± 29	118 ± 29	137 ± 9.9	113 ± 8.5	114 ± 16	134 ± 23
PAT-98-110	100	10.6 ± 0.30	60.0 ± 6.0	5.7 ± 0.6	116 ± 3.3	111 ± 12	138 ± 24	129 ± 34	128 ± 3.6	122 ± 13	113 ± 3.9	134 ± 6.5
PAT-98-111	90	9.70 ± 0.46	70.6 ± 12	7.3 ± 1.3	106 ± 5.0	131 ± 23	124 ± 22	158 ± 52	116 ± 5.5	144 ± 25	118 ± 18	141 ± 24
Moreno III												
LBA-02-46[c]	80	29.3 ± 0.67	141 ± 8.3	4.8 ± 0.3	**344** ± 7.9	**286** ± 20	<760 ± 310	536 ± 250	380 ± 8.7	318 ± 23	**315** ± 41	648 ± 160
LBA-02-48	29	13.7 ± 0.57	85.4 ± 8.1	6.2 ± 0.6	156 ± 6.5	166 ± 17	200 ± 38	215 ± 63	171 ± 7.1	183 ± 19	161 ± 7.2	207 ± 10
LBA-02-50	31–49	8.61 ± 0.32	57.3 ± 4.6	6.7 ± 0.6	96.7 ± 3.5	108 ± 9.7	111 ± 19	126 ± 32	106 ± 3.9	119 ± 11	103 ± 8.3	119 ± 10
LBA-02-51	50–71	11.5 ± 1.2	48.1 ± 4.9	4.2 ± 0.6	128 ± 13	89.2 ± 9.7	156 ± 33	100 ± 26	141 ± 14	98.1 ± 11	109 ± 28	128 ± 39
LBA-02-52	50–70	24.4 ± 1.5	ND	ND	279 ± 17	ND	512 ± 160	ND	307 ± 19	ND	279 ± –	512 ± –
Deseado I												
LBA-01-68	65	24.7 ± 0.64	142 ± 13	5.8 ± 0.6	270 ± 7.0	271 ± 27	477 ± 130	475 ± 210	297 ± 7.7	301 ± 30	271 ± 1.2	476 ± 1.3
LBA-01-73	25	9.01 ± 0.34	71.0 ± 4.5	7.9 ± 0.6	97.3 ± 3.6	131 ± 9.7	112 ± 19	158 ± 40	107 ± 4.0	144 ± 11	114 ± 24	135 ± 32

All samples measured at PRIME Lab except LBA-01-62 and 66 (Kaplan et al., 2004). Boulder heights with approximate sign are estimated based on photographs. Age1 calculated with local production rate (PR) and 0 mm/10^3 yr. Bold ages are oldest samples (Table 3). Age2 calculated with local production rate and average erosion rate of 1.4 mm/10^3 yr (Table 1). Age3 calculated with global production rates of Stone (2000) and no erosion. Individual boulder ages based on Age1 (No Erosion) and Age2 (Erosion), with the ^{10}Be and ^{26}Al measurements averaged; boulder age uncertainties are the standard deviation of the ^{10}Be and ^{26}Al ages. No shielding correction required. Attenuation length (Brown et al., 1992): 145 ± 7 g cm^{-2} (^{10}Be) and 156 ± 12 g cm^{-2} (^{26}Al). Procedural blanks: ^{10}Be = 5.60 and 4.10 × 10^{-15}; and ^{26}Al = 4.00 and 5.00 × 10^{-15}.

[a] Error includes analytical uncertainties (AMS and ICP-AES, the latter only for Al).

[b] Error includes propagation of analytical, production rate (~3%), erosion rate (~9% and 12% for ^{10}Be and ^{26}Al, respectively), and attenuation length (see above notes) uncertainties. Errors are propagated step-by-step while solving the age equation as explained in text.

[c] If an erosion rate of 1.4 mm/10^3 yr (Table 1) is used for the LBA-02-46 age determination, the solution is infinite. Thus, the Age2 of this sample is only known to be less than the 760,000 yr limit (Fig. 2).
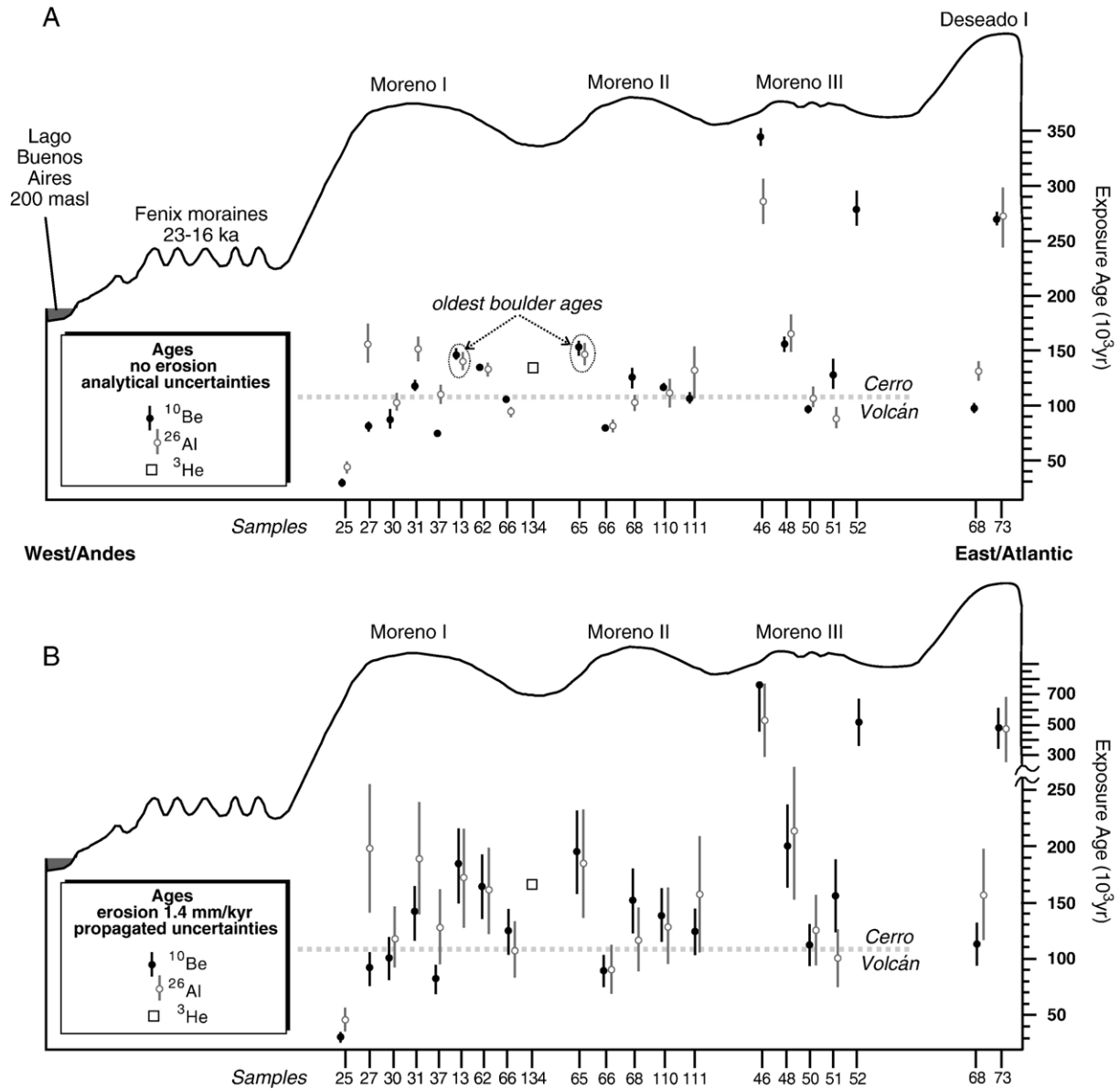
Figure 5. Schematic topographic profile from Lago Buenos Aires to Deseado I with new chronology. All ages ±1σ. Labels along the bottom of each figure refer to the last part of each sample id number and are in the same order left to right as in Table 2. Also shown is the 109,000 yr age for the Cerro Volcán flow that is (Fig. 2) stratigraphically above the Moreno complex (Singer et al., 2004). ³He data from Kaplan et al. (2004). (A) With Age1 from Table 2. (B). With Age2 from Table 2. No upper error bar is provided for LBA-02-46 because it must be <760,000 yr old (Table 2). Propagated uncertainties provide a possible age range for each boulder due to random uncertainties such as associated with erosion rate (~10%) and systematic uncertainties such as production rate (see text and Table 2).

necessarily be assumed a priori that the shortest boulders will be consistently the youngest. For example, although LBA-01-66 and LBA-02-25 are two of the shortest and youngest boulders (the latter clearly being exhumed), on the other hand, LBA-01-62 and PAT-98-13 are low samples and two of the oldest boulders on either Moreno I or II.

The exposure age distributions on Moreno III and Deseado I are distinct from the younger Moreno I and II moraines in that they contain three boulders with zero erosion ages that are >300,000 yr (Fig. 5A). Importantly, the younger ages (i.e., < ~200,000 yr) are from boulders from the lower end of the height range and they are similar to those on Moreno I and II (Table 2). For example, the younger Deseado

sample (LBA-01-73) is only 25 cm high and is much lower than the older LBA-01-68 boulder.

Ventifaction and other boulder surface relief features (Figs. 3D and F), and the spread in the age distribution, indicate that the assumption of zero erosion is unrealistic for all samples. Using an average erosion rate of 1.4 mm/10³ yr (Table 1) increases the boulder ages by ~11–26% (average ~17%), providing a potential age range for Moreno I and II from 178,000 to 105,000 and 190,000 to 90,000 yr, respectively. The ages of two boulders (LBA-02-25 and PAT-98-66) with an erosion rate of 1.4 mm/10³ yr are still significantly lower than the minimum age dictated by the Cerro Volcán basalt flow (Fig. 5B). For Moreno III, the

Table 3
Summary of Moreno boulder ages

Moraine	Without erosion			With erosion	
	Max ^{10}Be (10^3 yr)	Max ^{26}Al (10^3 yr)	Boulder age range (10^3 yr)	Mean of boulder ages (10^3 yr)	Boulder age range (10^3 yr)
Moreno I	146 ± 5	157 ± 17	143–92	141 ± 34	178–105
Moreno II	153 ± 6	148 ± 10	150–80	138 ± 35	190–90
Exclude PAT-98-66				150 ± 27	190–134
Moreno III	344 ± 8	286 ± 20	315–103	323 ± 242	648–119

Ages without erosion are based on Age1 in Table 2; the 1σ value is the analytical error for each age. Ages with erosion are based on Age2 in Table 2; the 1σ value is the standard deviation of all the boulder ages. For Moreno I, the arithmetic mean excludes the three samples with ^{26}Al/^{10}Be ratios >6 at the 95% confidence level; however, inclusion of these samples has no appreciable affect on the values (only 1000 yr).

boulder ages determined with the local erosion rate range from ca. 648,000 to 119,000 yr. For Deseado I, the ages are 476,000 and 135,000 yr.

For comparison, ages are presented based on Stone's (2000) production rates of 5.1 and 31.1 atoms/gm/yr (Age3 in Table 2; see Setting and methods), which differ by ~10% from ages calculated using the local rate. With these rates, the maximum ages with no erosion are 160,000 and 168,000 yr for Moreno I and II, respectively. Importantly, our main conclusions are unaffected by the choice of production rate (Fig. 6).

The production ratio of the two nuclides, ^{26}Al and ^{10}Be, should start off ~6 on relatively young surfaces and steadily decrease to less than 3 for ancient surfaces (Lal, 1991). Many boulders in Table 2 have high ^{26}Al/^{10}Be ratios (e.g., >8), which should not be possible by geologic processes (Lal, 1991). At 1σ, the percentage of ratios that is indistinguishable from 5 to 6 is only slightly less (60%) than expected from statistics alone (66%). However, four ratios are greater than 6 at even the 95% confidence level. The cause of the systematically high ratios remains uncertain. Alpha particles produced by U and Th decay could in theory produce excess ^{26}Al by the reaction ^{23}Na (α, n)^{26}Al (Sharma and Middleton, 1989). Also, we cannot rule out an underestimate of ^{9}Be concentration, perhaps due to contamination in the final processing steps, or an over-estimate of the measured ^{27}Al. If the high ratio samples (i.e., >6 at 2σ) are ignored, the findings of this study are unaffected for two reasons. First, the maximum boulder ages, which are used below to infer moraine ages (Table 3), have ratios of 5.5–6, the expected values. Second, exposure ages for boulders with ratios >6 are similar to those that have expected values (Table 2 and Fig. 5).

Discussion

Erosion rates

Erosion rates derived with old Telken boulder nuclide concentrations provide two important pieces of information essential to this study. First, the data indicate that the magnitude and variability of long-term erosion rates are remarkably low at LBA. The values are consistently less than ~2 mm/10^3 yr, for hornblende and feldspar rich granitic rocks

(Tables 1 and Appendix Table A1). These cosmogenic isotopic data and the geomorphology (Fig. 3; Singer et al., 2004) imply that the rocks at LBA are eroding slowly, consistent with preservation of glacial landforms that have survived for 1 myr. The erosion rates at LBA lie distinctly toward the lower end of values estimated in other semi-arid regions (0.5–12 mm/10^3 yr; see compilation by Small et al., 1997). The surface of the 109,000 yr old Cerro Volcán basalt flow also suggests minimal erosion in the LBA area. Although finer grained than the granitic rocks, this lava field still contains original pahoehoe surfaces (Ackert et al., 2003). Second, the Telken-based erosion rates allow an alternative method of estimating moraine age, without
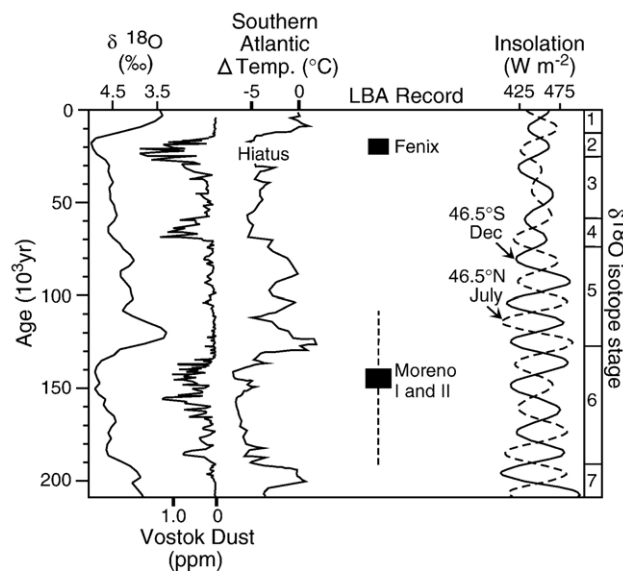

Figure 6. For the last ~200,000 yr, the LBA record compared with changes in the Northern Hemisphere ice sheets (i.e., δ^{18}O; Shackleton et al., 1990), Vostok dust concentration (Petit et al., 1998), southern ocean paleotemperature (Becquey and Gersonde, 2003), and changes in summer insolation in both hemispheres (Berger and Loutre, 1991). The dust has been isotopically fingerprinted to a Patagonian source with peak concentrations possibly corresponding to windblown material produced during glacial maxima (Basile et al., 1997). For LBA, the dashed line reflects the age range obtained for the two Moreno moraines, ca. 190,000–109,000 yr; the bottom of the line is the oldest boulder age with erosion and top of the line the Cerro Volcán lava flow age. The best estimate age for Moreno I and II (black square) is taken from Table 3 and for the Fenix moraine system from Kaplan et al. (2004). For comparison, with the production rates of Stone (2000), the oldest boulder ages (no erosion) for Moreno II and I are 168,000 and 160,000 yr, respectively.

having to rely exclusively on the assumption that erosion is negligible and the oldest boulders are most reliable (e.g., Putkonen and Swanson, 2003; Zreda and Phillips, 1995). The average and standard deviation of the erosion rates are 1.4 ± 0.8 mm/10^3 yr. The ~ 1 mm/10^3 yr variability could increase or decrease 150,000 yr surface exposure ages, as shown in Table 2, by up to ~ 12–15% or 15–22%, respectively. The standard deviation in erosion rate, which is >50% of the average, was not included in the propagation of age uncertainties (see Setting and methods) because then the total age errors would be unrealistically high given the nature of step-by-step error propagation.

The erosion rates shown in Table 1 are considered maxima for the respective Telken boulders for the following reason. The boulders were likely exhumed given the moraine ages of >760,000 yr, nuclide concentrations, and their heights of ~ 20–50 cm (Table 1). If erosion rates had been more than ~ 1.5–2 mm/10^3 yr, we infer that Telken granite boulders (and Deseado?) should be rare or nonexistent on the surface, as this would imply original heights for erratics >2 m, which are not found on younger deposits at LBA (Appendix Table A1 and Kaplan et al., 2004). Thus, the relatively common occurrence of boulders on the Telken moraines, and their given nuclide concentrations, suggest exhumation and the values in Table 1 are maxima.

Most or all of the Telken-based erosion rates could also be maxima for younger Moreno boulders. On the other hand, it must be kept in mind that erosion rates could have varied spatially and temporally over the LBA area over the last 1 myr and may have been higher for some Moreno boulders compared to the measured Telken erratics. For example, wind, one of the main elements of erosion, which is evident in ventifaction (Fig. 3D), may not have had a constant speed over the region as topography varies (Figs. 2 and 5).

The boulder erosion rates in Table 1 can be used to judge the magnitude of moraine erosion and boulder exhumation, key processes that may have affected exposure ages shown in Table 2. Available evidence indicates that, in general, boulders erode slower than their surrounding landscape (e.g., Granger et al., 2001), thus the erosion rates presented here may be less than that for the moraine matrix. Taking the maximum boulder erosion rate of 2.4 mm/10^3 yr (in Table 1) as a minima for the moraine matrix, then in $\sim 150,000$ yr at least 0.4 m of Moreno I and II (see below) and ~ 2 m of each Telken moraine have eroded away. Based on this simple analysis, it is assumed that all Telken (and Deseado?) boulders have been exhumed and most or all Moreno II boulders have been at the surface since deposition. Many Moreno I and III boulders could also have been exhumed, agreeing with the observation that the tallest boulders are generally the oldest, at least for the latter moraine. Exhumation rates likely vary depending on slope and aspect with respect to dominant wind directions. Moraines (and boulders) are expected to be eroding at different rates, including outside of the range shown in Table 1, leading to differential exhumation. For example, boulders on Telken V and VII could have been

exposed less time than those on the younger Telken IV (see ages with no erosion in Table 1), accounting for lower isotope concentrations and higher apparent erosion rates (Fig. 4).

Gillespie and Bierman (1995) highlighted that time and erosion rate could potentially be solved uniquely with two measured isotopes (i.e., Lal, 1991; two equations and two unknowns). Such analyses on the Telken data produce a range of values consistent with those presented in Table 1. However, the production rate, half-lives of ^{10}Be and ^{26}Al (1.50 and 0.72 myr, respectively), exposure duration, and analytic and geologic uncertainties prevent a unique solution for both unknowns.

Glacial chronology

For moraines of Moreno and Deseado age, >100,000 yr, the question arises, how do boulder ages relate to moraine age? The standard deviation of all the boulder ages for each moraine is much higher than the analytical uncertainties of the ^{10}Be and ^{26}Al ages, which are commonly less than 4% for the former (Tables 2 and 3). The age variability shown in Figure 5 likely reflects spatial–temporal and lithologic differences in erosion rates and exhumation. Given that most geologic processes cause a lowering of apparent exposure ages, the consensus is that, assuming no erosion, the oldest cosmogenic exposure age (Table 3) best represents the true moraine age (Hallet and Putkonen, 1994; Putkonen and Swanson, 2003; Zreda and Phillips, 1995). Because erosion must be >0 mm/10^3 yr, even if by an insignificant amount, the oldest exposure ages should provide (close?) minimum ages for the moraines. We also present exposure ages calculated with erosion as a supporting approach to assessing moraine age (Age2 in Tables 2 and 3). An average erosion rate of 1.4 mm/10^3 yr is used in the age equation assuming that, whereas this rate may be a maximum for some Moreno boulders it is a minimum for others.

Moreno I and II

The age distributions for Moreno I and II are clearly indistinguishable even considering analytical uncertainties (Fig. 5). The maximum boulder ages with no erosion (PAT-98-13 and 65; Fig. 5A) are 143,000 and 150,000 for Moreno I and II; the individual ^{10}Be and ^{26}Al ages are indistinguishable at 1σ for each respective boulder, even within analytical uncertainty (Fig. 5A). Considering erosion, the boulder ages for Moreno I and II range from 178,000 to 105,000 yr and 190,000 to 90,000 yr (oldest ages are $\pm$ $\sim 10,000$ yr; Table 2), respectively. However, the Cerro Volcán ^{40}Ar/^{39}Ar age provides a minimum constraint of 109,000 yr for both moraines. The standard deviation of all boulder ages is $\sim 20,000$–35,000 yr (Tables 2 and 3).

The two approaches used to refine the estimated time of deposition between $\sim 190,000$ and 109,000 yr–the maximum age with no erosion and mean age of all boulders with erosion–both provide the same result (Table 3). For Moreno I, the mean boulder age considering erosion is 141,000 yr,

similar to the maximum age with no erosion. The mean boulder age in Table 3 does not include the three samples from Moreno I that have ^{26}Al/^{10}Be ratios >6 at the 95% confidence level. However, if these 3 samples are included in the mean, they have no appreciable affect on the value, 140,000 yr. For Moreno II, the mean age of all boulders considering erosion is 138,000 yr, which is slightly less than the maximum age with no erosion. However, the average age of all boulders incorporates PAT-98-66, which is the only Moreno boulder age (with erosion) statistically below the 109,000 yr old Cerro Volcán age constraint. In addition, the PAT-98-66 boulder age is more than 1σ different than the other Moreno II boulder ages (Table 2). As discussed above, PAT-98-66 is the shortest Moreno II boulder and it could have been exhumed, or the Telken-based erosion rate underestimates how fast this erratic is disintegrating. If PAT-98-66 is excluded from the average, the age with erosion for Moreno II is 150,000 yr, identical to the maximum boulder age of 150,000 yr with no erosion (Table 3).

Taken at face value, Moreno II is ~10,000 years older than Moreno I (Table 3), which is consistent with their relative positions, based on either the maximum boulder ages (0 mm/ 10^3 yr) or average age with erosion if PAT-98-66 is considered an outlier. However, these moraines cannot be statistically differentiated in time given available data; nonetheless, Moreno I and II clearly relate to the same glaciation (Fig. 6). If the Telken-based erosion rates are, in general, maxima for the younger Moreno moraines, than the erosion rate corrected ages could be upper limits. On the other hand, the similarity between the average age with erosion and the maximum ages with no erosion (140,000–150,000 yr) may indicate that use of an 'average' rate of 1.4 mm/10^3 yr (half of the Telken samples have values between 0.8 and 1.2 mm/10^3 yr) is representative of at least some Moreno boulders.

Moreno III and Deseado I

Preliminary ages of the Moreno III and Deseado I moraines can be inferred from data in Table 2. These age ranges are independent of whether global (Gosse and Stone, 2001) or local production rates are used, which are ~11% different. The maximum ages of Moreno III and Deseado I are 760,000 yr, constrained by the stratigraphically older ^{40}Ar/^{39}Ar dated Arroyo Page Flow (Fig. 2). The minimum moraine age for Moreno III, obtained from the oldest exposure age with no erosion (Fig. 5A) (cf., Zreda and Phillips, 1995), may be 315,000 ± 41,000 yr. Similarly, the exposure ages suggest a minimum age for Deseado I of 271,000 ± 1,200 yr. However, Deseado I is older than Moreno III (Fig. 2), and thus it also must be >315,000 ± 41,000 yr. The two oldest zero erosion Moreno III ages are more than 125,000 yr older than any boulder from the younger Moreno I and II moraines. For the sake of argument, assuming an erosion rate less than half of that derived here (Fig. 4), e.g., ~0.5 mm/10^3 yr, the modeled ages of the oldest erratics on Moreno III and Deseado I would be at least 400,000–300,000 yr.

This interpretation, i.e., Moreno III is much older than Moreno I and II, implies that the boulders (LBA-02-48, 50, and 51) yielding young exposure ages have been exhumed. The highest boulders on Moreno III and Deseado I are also the oldest. Moreno III may mark a retreat position from the Deseado I advance. In this case, younger Moreno III ages could reflect re-working by subsequent glacio-fluvial erosion, and hence they produce a broadly similar age range as Moreno I and II, <200,000 yr. If exhumation explains the younger Moreno III ages, then Table 2 suggests that boulders should be at least ~70 cm high for dating old erratics on this moraine.

Alternatively, inheritance from prior cosmic ray exposure could be invoked to explain the two oldest ages on Moreno III. The two oldest boulders could have been reworked from a much older moraine during the later glacial event. If the oldest boulders are from a prior glaciation, then Moreno III would be part of the same glaciation as the younger Moreno I and II deposits. Also, the older samples may contain accumulated atoms from exposure prior to incorporation into the ice. However, given the available evidence, it is not apparent that such a large amount of inheritance, >100,000 yr of previous exposure in the case of Moreno III, has had an important effect on other Moreno moraines, the 5 distinct younger Fenix moraines <25,000 yr old (Kaplan et al., 2004), or elsewhere in the world (see Putkonen and Swanson, 2003). Resolution of this question requires further dating.

Comparison with marine oxygen isotope stages

The exposure age ranges indicate that the Moreno I and II moraines were deposited during a major expansion of Patagonian ice during marine oxygen isotope stage 6 (Fig. 6). The maximum boulder ages with no erosion, ca. 150,000–140,000 yr, overlap with the heaviest marine δ^{18}O values and thus largest Northern Hemisphere ice volume and coldest southern ocean temperatures (Fig. 6), suggesting a glacial maximum late in stage 6. With erosion, the distribution and average of exposure ages also support a stage 6 glaciation. The timing of maximum ice expansion at LBA also overlaps with peak glacial-age dust concentration in Antarctic ice (Fig. 6), which has a distinct Patagonian Sr, Nd, and Pb isotope signature (Basile et al., 1997; Petit et al., 1998). The range of exposure ages of Moreno I and II and the limiting age provided by the Cerro Volcán flow allow the possibility that the moraines correspond to stage 5d (Fig. 5). However, we consider a 5d age for Moreno moraines unlikely, as most of the measured boulders have been exposed much longer than 115,000 yr (Fig. 5) and there is no evidence for a major glaciation at this time recorded by dust in Antarctic ice (Fig. 6).

The next major glaciation documented at LBA occurred between ca. 23,000 and 16,000 yr ago (Kaplan et al., 2004). Thus, the last two glacial maxima recorded at LBA were during stages 6 and 2. Confirming an earlier finding (Kaplan et al., 2004), glacial deposits dating to stage 4 were not found despite a peak in dust concentration at Vostok (Fig.

6). If a glacial event occurred during stage 4, the deposits were removed by the subsequent ice advances during the last glacial maximum. These results are consistent with the volcanic geology at the 3600-m-high Tatara–San Pedro complex (Fig. 1) in the southern Andes at 36°S. There, prominent gaps in the lava record during stages 6 and 2 are thought to reflect major episodes of glacial erosion, and furthermore, glaciation during stage 4 appears to have been less intense (Singer et al., 1997).

The ages of the three oldest erratics on Moreno III and Deseado I may suggest that the glaciation that they reflect was at least two glacial cycles (325,000–190,000 yr ago) before Moreno II (Fig. 7). If correct, a possible implication is that a stage 8 glaciation (275,000–250,000 yr ago) occurred, but is not preserved at LBA. Interestingly, stage 8 is much smaller than stages 2, 6, 10, and 16 in terms of Northern Hemisphere ice sheet volume (Shackleton et al., 1990). There is a prominent peak in dust concentration at Vostok at ~250,000 yr ago (Fig. 7). If a stage 8 glaciation occurred at LBA as implied by the ice core data (Fig. 7), and the associated deposits are not preserved at LBA, then they may have been subsequently removed by the younger glacial events, analogues to the stage 4 deposits. Additional boulder analyses underway will refine the age estimates and test this hypothesis.

Conclusions

Cosmogenic nuclide measurements allow direct dating of moraines in the middle latitudes of the Southern Hemisphere to stage 6, well beyond the limits of the radiocarbon method. Accurate age determinations on Patagonian moraines as old as 150,000 yr are possible because integrated rates of erosion are low. On the basis of nuclide concentrations in erratics

deposited prior to a lava flow that is $^{40}Ar/^{39}Ar$ dated at 760,000 yr, the maximum rate of erosion on old moraines is constrained to be <2 mm/10^3 yr. The exposure age chronology suggests that ice expanded onto the Patagonian plains east of the Andean cordillera and left well-preserved moraines at least once between 760,000 and 200,000 yr ago. The next recorded glaciation occurred within the age range from ~190,000 to 109,000 yr ago. The maximum exposure ages assuming no erosion and average age with an erosion correction provide a best estimate of 150,000–140,000 yr for maximum ice expansion. Subsequently, ice left well-preserved moraine belts during stage 2. Apparently, moraines corresponding to stage 4 are not preserved at Lago Buenos Aires (LBA). Most likely, they were overrun and removed by ice during the more prominent advances associated with stage 2. A major implication is that not only did major ice advances in the southern mid-latitudes coincide in timing with Northern Hemisphere ice expansions during at least the last ~200,000 yrs, but the relative magnitude of areal extent during stages 6, 4, and 2 was similar as well. Specifically, in the Northern Hemisphere, stage 6 moraines are often, although not always, slightly less extensive than stage 2, and stage 4 is often the least extensive or not recorded (e.g., Phillips et al., 1997). Subject to additional analyses, we also hypothesize that a stage 8 glaciation occurred but is not preserved at LBA, and was obliterated by the subsequent stage 6 advance. Additional cosmogenic ages will be helpful in constraining the age of LBA moraines prior to stage 6.

The Moreno I and II and Fenix ages, ca. 150,000–140,000 yr and 23,000–16,000 yr (Fig. 6), specifically imply that: (1) during at least the last two 100,000 yr glacial cycles, southern Andean and Northern Hemisphere glaciations were coeval and in the mid- to late Quaternary Period interhemispheric synchronicity of glacial maxima is the rule and not the
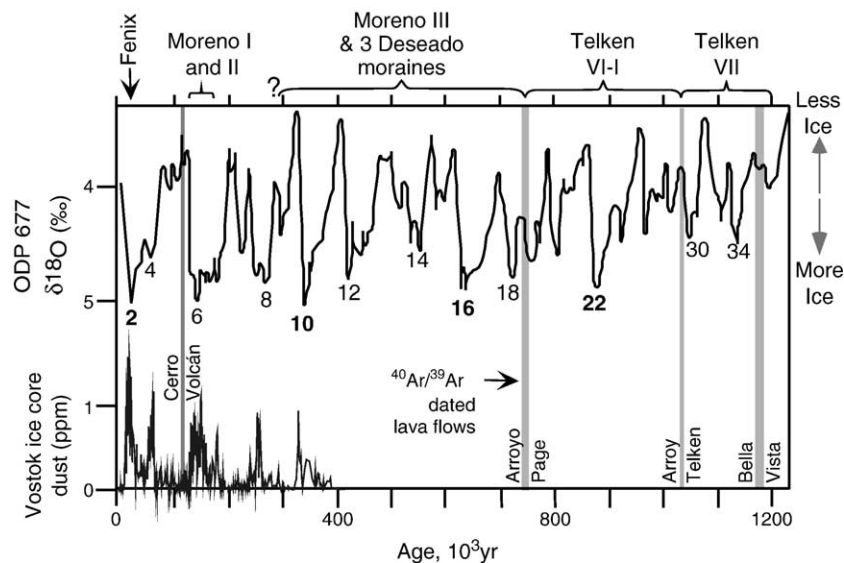

Figure 7. After Singer et al. (2004). Comparison of moraine record and lava flow age constraints with orbitally-tuned record of Shackleton et al. (1990). The dust concentration from Vostok ice is from Petit et al. (1998). Note that no LBA moraines corresponding to stage 4 (and tentatively stage 8) have been found, despite a peak in Patagonian-derived dust in Antarctica.

exception; (2) the 100,000-yr eccentricity-based periodicity paces ice volume change in the middle latitudes of both hemispheres despite out-of-phase insolation, causing global ice age maxima (Imbrie et al., 1993). A global ice-sheet system interlocked by sea level and climate change has been proposed to explain Southern Hemisphere glacial history, including the Antarctic (Denton et al., 1986). Theories of ice age climate must continue to clarify how relatively small changes in the distribution of the sun's energy in the Northern Hemisphere strongly influenced the past behavior of middle latitude Southern Hemisphere mountain glaciers.

Acknowledgments

Appendix

Table A1
Description of samples and scaling factors used

Sample	Elevation (km)	Sample thickness (cm)	Latitude °S (DD.MM)	Longitude °W (DD.MM)	Scaling factors				Quartz dissolved (gm)	Be added (mg)	Rock type
					Local rate[a]		Global rate[b]				
					^{10}Be	^{26}Al	^{10}Be	^{26}Al			
Moreno I											
LBA-02-25	0.511	1.3	46 32.940	70 52.941	9.3516	57.1235	8.5386	52.1628	28.699	0.5665	hornblende rich granite
LBA-02-27	0.503	1.3	46 32.933	70 52.974	9.2859	56.7216	8.4782	51.7929	24.631	0.4095	pink granite
LBA-02-30	0.520	1.5	46 33.291	70 53.076	9.4113	57.4949	8.5936	52.5051	11.986	0.2869	hornblende rich granite
LBA-02-31	0.494	1.8	46 33.831	70 53.096	9.1792	56.0838	8.3802	51.2075	22.565	0.4182	pink granite
LBA-02-37	0.495	0.9	46 32.789	70 53.104	9.2591	56.5409	8.4533	51.6251	29.418	0.3664	pink granite
PAT-98-13	0.503	1.5	46 34.570	70 52.887	9.274	56.6547	8.4673	51.7320	28.974	0.4375	pink granite
LBA-01-62	0.457	1.5	46 37.465	70 54.542	8.9075	54.4127	8.1301	49.6689	37.200	0.4905	quartz vein in metamorphic rock
LBA-01-66	0.475	1.5	46 37.950	70 55.490	9.0524	55.2993	8.2634	50.4847	42.470	0.5003	quartz vein in metamorphic rock
Moreno II											
PAT-98-65	0.507	1.5	46 34.471	70 51.646	9.3065	56.8536	8.4972	51.9150	20.922	0.3982	pink granite
PAT-98-66	0.518	3.0	46 34.431	70 51.655	9.2693	56.6813	8.4639	51.7614	32.739	0.3870	pinkish gray granite
PAT98-068	0.535	1.5	46 32.633	70 52.412	9.5366	58.2614	8.7089	53.2104	36.39	0.3982	Granite
PAT-98-110	0.513	1.5	46 34.448	70 51.409	9.3554	57.1529	8.5422	52.1904	11.53	0.3124	Pink tuff, quartz rich
PAT-98-111	0.518	1.5	46 34.430	70 51.660	9.3963	57.4034	8.5799	52.4208	8.243	0.3168	pink granite
Moreno III											
LBA-02-46	0.497	1.8	46 33.785	70 50.011	9.2065	56.2510	8.4053	51.3613	30.340	0.4453	pink granite
LBA-02-48	0.502	3.5	46 33.488	70 50.721	9.0979	55.6496	8.3065	50.8138	14.077	0.3453	gray rhyolite
LBA-02-50	0.509	4.0	46 33.659	70 50.376	9.1100	55.7416	8.3179	50.9001	19.905	0.3973	hornblende rich granite
LBA-02-51	0.494	1.3	46 32.397	70 50.457	9.2234	56.3363	8.4206	51.4381	11.201	0.3453	hornblende rich granite
LBA-02-52	0.505	1.0	46 32.387	70 50.741	9.3310	56.9849	8.5194	52.0341	9.811	0.3433	pink granite
Deseado I											
LBA-01-68	0.557	1.5	46 40.955	70 52.378	9.7194	59.3800	8.8771	54.2396	32.531	0.3875	pinkish gray granite
LBA-01-73	0.526	1.5	46 40.833	70 51.685	9.4652	57.8248	8.6433	52.8086	26.264	0.3801	granite
Telken IV											
LBA-02-34	0.660	2.3	46 29.148	70 35.381	10.5429	64.4533	9.6352	58.9099	25.261	0.4012	pink granite

Table A1 (continued)

Sample	Elevation (km)	Sample thickness (cm)	Latitude °S (DD.MM)	Longitude °W (DD.MM)	Scaling factors				Quartz dissolved (gm)	Be added (mg)	Rock type
					Local rate[a]		Global rate[b]				
					^{10}Be	^{26}Al	^{10}Be	^{26}Al			
LBA-02-36	0.655	1.5	46 29.214	70 35.830	10.5803	64.6470	9.6691	59.0853	30.038	0.3914	pink granite
Telken V											
LBA-01-48	0.631	2.5	46 53.381	70 43.529	10.2659	62.7643	9.3804	57.3565	7.650	0.3531	hornblende rich granite
Telken VII											
LBA-02-42	0.632	2.0	46 53.192	70 43.417	10.3186	63.0665	9.4286	57.6330	3.753	0.2979	hornblende rich granite
PAT-98-108	0.635	1.7	46 50.245	70 43.603	10.3833	63.4488	9.4880	57.9836	21.951	0.3943	red rhyolite

Scaling factors include correction for sample thickness in the third column.

[a] Local rate based on Ackert et al. (2003). See Setting and methods section.

[b] Global rate is from Stone (2000), corrected for atmospheric pressure of 1009.32 mbar and temperature of 285 K.

References

Ackert, R.P., Singer, B.S., Guillou, H., Kaplan, M.R., Kurz, M.D., 2003. Long-term cosmogenic ^{3}He production rates from $^{40}Ar/^{39}Ar$ and K–Ar dated Patagonian lava flows at 47°S. Earth and Planetary Science Letters 210, 119–136.

Basile, I., Grousset, F.E., Revel, M., Petit, J.R., Biscaye, P.E., Barkov, N.I., 1997. Patagonian origin of glacial dust deposited in East Antarctica (Vostok and Dome C) during glacial stages 2, 4, and 6. Earth and Planetary Science Letters 146, 573–589.

Becquey, S., Gersonde, R.A., 2003. 0.55-Ma paleotemperature record from the Subantarctic zone: implications for Antarctic circumpolar current development. Paleoceanography 18 (doi:10.1029/2000PA000576).

Berger, A., Loutre, M.F., 1991. Insolation values for the climate of the last 10 million years. Quaternary Science Reviews 10, 297–318.

Bierman, P.R., Caffee, M.W., Davis, P.T., Marsella, K., Pavich, M., Colgan, P., Mickelson, D., 2002. Rates and timing of earth surface processes from in situ-produced cosmogenic Be-10. In: Grew, E.S. (Ed.), Beryllium: Mineralogy, Petrology, and Geochemistry. Series: Reviews in Mineralogy and Geochemistry, vol. 50. Mineralogical Society of America, Washington, DC, pp. 147–205.

Broecker, W.S., Denton, G.H., 1989. The role of ocean–atmosphere reorganizations in glacial cycles. Geochimica et Cosmochimica Acta 53, 2465–2501.

Brook, E.J., Kurz, M.D., Ackert Jr., R.P., Denton, G.H., Brown, E.T., Raisbeck, G.M., Yiou, F., 1993. Chronology of Taylor Glacier advances in Arena Valley, Antarctica, using in situ cosmogenic ^{3}He and ^{10}Be. Quaternary Research 39, 11–23.

Brown, E.T., Brook, E.J., Raisbeck, G.M., Yiou, F., Kurz, M.D., 1992. Effective attenuation of cosmic rays producing ^{10}Be and ^{26}Al in quartz: implications for exposure dating. Geophysical Research Letters 19, 369–372.

Caldenius, C.G., 1932. Las glaciaciones Cuaternarias en la Patagonia and Tierra del Fuego. Geografiska Annaler 14, 1–164.

Clapperton, C.M., 1993. Quaternary Geology and Geomorphology of South America. Elsevier.

Denton, G.H., Hughes, T.J., Karlén, W., 1986. Global ice-sheet system interlocked by sea level. Quaternary Research 26, 3–26.

Gillespie, A.R., Bierman, P.R., 1995. Precision of terrestrial exposure ages and erosion rates from analysis of cosmogenic isotopes produced in situ. Journal of Geophysical Research 100, 24637–24649.

Gosse, J.C., Phillips, F.M., 2001. Terrestrial in situ cosmogenic nuclides: theory and application. Quaternary Science Reviews 20, 1475–1560.

Gosse, J.C., Stone, J.O., 2001. Terrestrial cosmogenic nuclide methods passing milestones toward paleo-altimetry. EOS 82, 82, 86, 89.

Granger, D.E., Riebe, C.S., Kirchner, J.W., Finkel, R.C., 2001. Modulation of erosion on steep granitic slopes by boulder armoring, as revealed by cosmogenic ^{26}Al and ^{10}Be. Earth and Planetary Science Letters 186, 269–281.

Hallet, B., Putkonen, J.K., 1994. Surface dating of dynamic landforms. Young boulders on aging moraines. Science 265, 937–940.

Hays, J.D., Imbrie, J., Shackleton, N.J., 1976. Variations in the earth's orbit: pacemaker of the ice ages. Science 194, 1121–1131.

Imbrie, J., Berger, A., Boyle, E.A., Clemens, S.C., Duffy, A., Howard, W.R., Kukla, G., Kutzbach, J., Martinson, D.G., McIntyre, A., Mix, A.C., Molfino, B., Morley, J.J., Peterson, L.C., Pisias, N.G., Prell, W.L., Raymo, M.E., Shackleton, N.J., Toggweiler, J.R., 1993. On the structure and origin of major glaciation cycles 2. The 100,000-year cycle. Paleoceanography 8, 699–735.

Kaplan, M.R., Ackert, R.P., Singer, B.S., Douglass, D.C., Kurz, M.D., 2004. Cosmogenic nuclide chronology of millennial-scale glacial advances during O-isotope Stage 2 in Patagonia. Geological Society of America Bulletin 116, 308–321.

Lal, D., 1991. Cosmic ray labeling of erosion surfaces: in-situ nuclide production rates and erosion models. Earth and Planetary Science Letters 104, 424–439.

Licciardi, J.M., Kurz, M.D., Clark, P.U., Brook, E.J., 1999. Calibration of cosmogenic ^{3}He production rates from Holocene lava flows in Oregon, USA, and effects of the Earth's magnetic field. Earth and Planetary Science Letters 172, 261–271.

Masarik, J., Frank, M., Schäfer, J.M., Wieler, R., 2001. Correction of in situ cosmogenic nuclide production rates for geomagnetic field intensity variations during the past 800,000 years. Geochimica et Cosmochimica Acta 65, 2995–3003.

Mercer, J.H., 1983. Cenozoic glaciation in the southern hemisphere. Annual Reviews of Earth and Planetary Science 11, 99–132.

Middleton, R., Brown, L., Dezfouly-Arjomandy, B., Klein, J., 1993. On ^{10}Be standards and the half life of ^{10}Be. Nuclear instruments and methods in physics research B82, 399–403.

Mörner, N.-A., Sylwan, C., 1989. Magnetostratigraphy of the Patagonian moraine sequence at Lago Buenos Aires. Journal of South American Earth Sciences 2, 385–389.

Nishiizumi, K., Winterer, E.L., Kohl, C.P., Klein, J., Middleton, R., Lal, D., Arnold, J.R., 1989. Cosmic ray production rates of ^{10}Be and ^{26}Al in quartz from glacially polished rocks. Journal of Geophysical Research 94, 17907–17915.

Partridge, T.C., Granger, D.E., Caffee, M.W., Clarke, R.J., 2003. Lower Pliocene hominid remains from Sterkfontein. Science 300, 607–612.

Petit, J.R., Jouzel, J., Raynaud, D., Barkov, N.I., Barnola, J.M., Basile, I., Bender, M., Chappellaz, J., Davis, M., Delaygue, G., Delmotte, M.,

Kotlyakov, V.M., Legrand, M., Lipenkov, V.Y., Lorius, C., Pépin, L., Ritz, C., Saltzman, E., Stievenard, M., 1998. Climate and atmospheric history of the past 420,000 years from the Vostok ice core, Antarctica. Nature 399, 429–436.

Phillips, F.M., Zreda, M.G., Gosse, J.C., Klein, J., Evenson, E.B., Hall, R.D., Chadwick, O.A., Sharma, P., 1997. Cosmogenic ^{36}Cl and ^{10}Be ages of Quaternary glacial and fluvial deposits of the Wind River Range, Wyoming. Geological Society of America Bulletin 109, 453–1463.

Putkonen, J., Swanson, T., 2003. Accuracy of cosmogenic ages for moraines. Quaternary Research 59, 255–261.

Shackleton, N.J., Berger, A., Peltier, W.R., 1990. An alternative astronomical calibration of the lower Pleistocene timescale based on ODP site 677. Transactions of the Royal Society of Edinburgh. Earth Sciences 81, 251–261.

Shanahan, T.M., Zreda, M., 2000. Chronology of Quaternary glaciations on Mount Kenya and Kilimanjaro. Earth and Planetary Science Letters 177, 23–42.

Sharma, P., Middleton, R., 1989. Radiogenic production of ^{10}Be and ^{26}Al in uranium and thorium ores: implications for studying terrestrial samples containing low levels of ^{10}Be and ^{26}Al. Geochimica et Cosmochimica Acta 53, 709–716.

Singer, B.S., Thompson, R.A., Dungan, M.A., Feeley, T.C., Nelson, S.T., Pickens, J.C., Brown, L.L., Wulff, A.W., Davidson, J.P., Metzger, J., 1997. Volcanism and erosion during the past 930 thousand years at the Tatara–San Pedro complex, Chilean Andes. Geological Society of America Bulletin 109, 127–142.

Singer, B.S., Ackert, R.P., Guillou, H., 2004. ^{40}Ar/^{39}Ar and K–Ar chronology of Pleistocene glaciations in Patagonia. Geological Society of America Bulletin 116, 434–450.

Small, E.E., Anderson, R.S., Repka, J.R., Finkel, R., 1997. Erosion rates of alpine bedrock summit surfaces deduced from in situ ^{10}Be and ^{26}Al. Earth and Planetary Science Letters 150, 413–425.

Stone, J.O., 2000. Air pressure and cosmogenic isotope production. Journal of Geophysical Research 105, 23753–23759.

Sugden, D.E., Hulton, N.R.J., Purves, R.S., 2002. Modelling the inception of the Patagonian icesheet. Quaternary International 95/96, 55–64.

Taylor, J.R., 1982. An Introduction to Error Analysis. University Science Books, Mill Valley, California.

Zreda, M.G., Phillips, F.M., 1995. Insights into alpine moraine development from cosmogenic ^{36}Cl buildup dating. Geomorphology 14, 149–156.